Available online at www.sciencedirect.com
SCIENCE DIRECT®
Journal of Structural Biology 143 (2003) 229–241
Journal of Structural Biology
www.elsevier.com/locate/yjsbi

The molecular deposition of transgenically modified starch in the starch granule as imaged by functional microscopy

Andreas Blennow,[a,*] Michael Hansen,[b] Alexander Schulz,[b] Kirsten Jørgensen,[a] Athene M. Donald,[c] and James Sanderson[c]

[a] *Center for Molecular Plant Physiology, Plant Biochemistry Laboratory, Department of Plant Biology, The Royal Veterinary and Agricultural University, 40 Thorvaldsensvej, DK-1871 Frederiksberg C, Copenhagen, Denmark*
[b] *Plant Physiology and Anatomy Laboratory, Department of Plant Biology, The Royal Veterinary and Agricultural University, 40 Thorvaldsensvej, DK-1871 Frederiksberg C, Copenhagen, Denmark*
[c] *The Polymers and Colloids group, Department of Physics, University of Cambridge, Cavendish Laboratory, Madingley Rd, Cambridge, CB3 0HE, UK*

Received 16 April 2003, and in revised form 21 August 2003

Abstract

The molecular deposition of starch extracted from normal plants and transgenically modified potato lines was investigated using a combination of light microscopy, environmental scanning electron microscopy (ESEM) and confocal laser scanning microscopy (CLSM). ESEM permitted the detailed (10 nm) topographical analysis of starch granules in their hydrated state. CLSM could reveal internal molar deposition patterns of starch molecules. This was achieved by equimolar labelling of each starch molecule using the aminofluorophore 8-amino-1,3,6-pyrenetrisulfonic acid (APTS). Starch extracted from tubers with low amylose contents (suppressed granule bound starch synthase, GBSS) showed very little APTS fluorescence and starch granules with low molecular weight amylopectin and/or high amylose contents showed high fluorescence. Growth ring structures were sharper in granules with normal or high amylose contents. High amylose granules showed a relatively even distribution in fluorescence while normal and low amylose granules had an intense fluorescence in the hilum indicating a high concentration of amylose in the centre of the granule. Antisense of the starch phosphorylating enzyme (GWD) resulted in low molecular weight amylopectin and small fissures in the granules. Starch granules with suppressed starch branching enzyme (SBE) had severe cracks and rough surfaces. Relationships between starch molecular structure, nano-scale crystalline arrangements and topographical–morphological features were estimated and discussed.

Keywords: *Solanum tuberosum*; Antisense suppression; Starch granule; Amylose; Amylopectin; Confocal laser scanning microscopy; Environmental scanning electron microscopy

1. Introduction

Starch is the most important energy reserve in higher plants. Storage starch is accumulated in storage organs like tubers or seeds over long time periods, which allows the formation of large (approx 10–100 μm) granular structures in the plastids. The deposition of starch molecules and the formation of organised starch granules are complex processes governed by a combination of the enzyme activities that are directly involved in starch chain elongation, branching and phosphate substitution and hydrolytic activities as well as the physical self-assembly and side-by-side packing of newly synthesised α-glucan double helical motifs (Smith, 2001). Normal storage starch is a mixture of 20–30% amylose consisting of nearly linear chains of glucose units linked by α-1,4 glucosidic bonds and 70–80% amylopectin, having an α-1,4 backbone structure and approx. 5% of α-1,6 glucosidic branch points. Amylopectin is a much larger molecule ($1–2 \times 10^8$ g mol^{-1}) than amylose (10^6 g mol^{-1}), (Blennow et al., 2001). The α-1,6 glucosidic branch points in amylopectin permit the efficient

* Corresponding author. Fax: +45-35-28-33-33.
E-mail address: abl@kvl.dk (A. Blennow).

1047-8477/$ - see front matter © 2003 Elsevier Inc. All rights reserved.
doi:10.1016/j.jsb.2003.08.009

crystalline packing of the α-glucan chains in the starch granules and also provide non-reducing ends to be further elongated, thereby stimulating starch biosynthesis. Hence, amylopectin is important for efficient formation of normal starch granules. Amylose does not form a crystalline lattice like the amylopectin does but is deposited as mainly non-crystalline chains in the granule (Buléon et al., 1998). However, various extents of amylose–amylopectin interactions (Jane et al., 1992; Kasemsuwan, 1994; Obanni and BeMiller, 1997) may affect starch granule integrity (Jenkins and Donald, 1995). The only known *in planta* modification of starch is starch phosphorylation (Blennow et al., 2002). The phosphate groups are found monoesterified at the C-3 and the C-6 positions of a small fraction (ca. 0.1%) of the glucose units of amylopectin (Blennow et al., 1998). Phosphate monoesters are present in crystalline parts of the starch granules (Blennow et al., 2000b) and may affect crystallinity and integrity of the starch granules (Blennow et al., 2002; Muhrbeck et al., 1991) but the effects of phosphate on starch molecular packing is not clear.

Based on a variety of starch structural data, a plausible model of the starch granule at several levels of organisation has been suggested (Gallant et al., 1997), (Fig. 1). The chain length profiles of amylopectin obtained after enzymatic debranching and subsequent chromatographic separation of the unit chains reveals a polymodal distribution of the chains (Manners, 1989). suggestsing a clustered organisation of the chains in the starch granule. Based on powder and fibre X-ray diffraction data and molecular modelling, the amylopectin molecular chains form parallel, dense, left handed double helices with 6 glucose residues per turn and a 2.1 nm pitch. In the starch granule, these double helices are 5–8 nm long and the two chains in a double helix are linked and thereby stabilised at the reducing side by an α-1,6 branch point. The double helices can be considered as stable mesogens packed in the granule as concentric crystalline lamellae interrupted by 1–4 nm amorphous lamellae containing the branch points (Waigh et al., 1998). The lamellae have a constant 9 nm repeat structure as determined by small angle X-ray scattering (SAXS, Jenkins et al., 1993). The double helices can align in two different crystalline lattices, the A-type

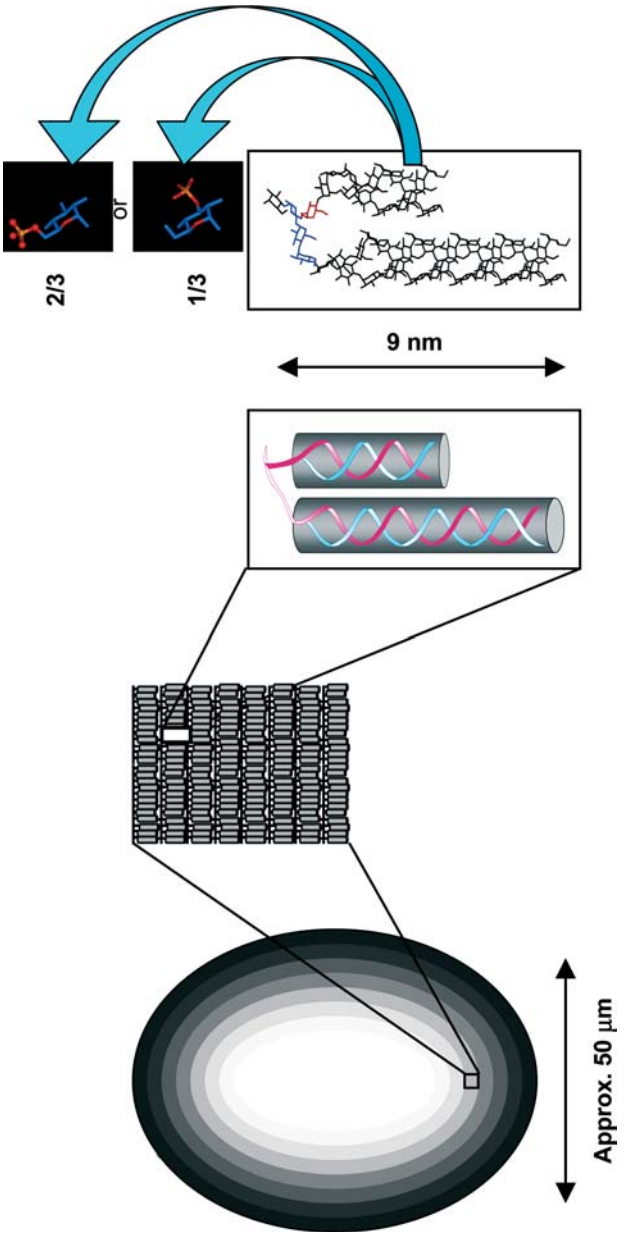

Fig. 1. Schematic representation of a starch granule at different levels of organisation proposed by Gallant et al. (1997). See text for further details.

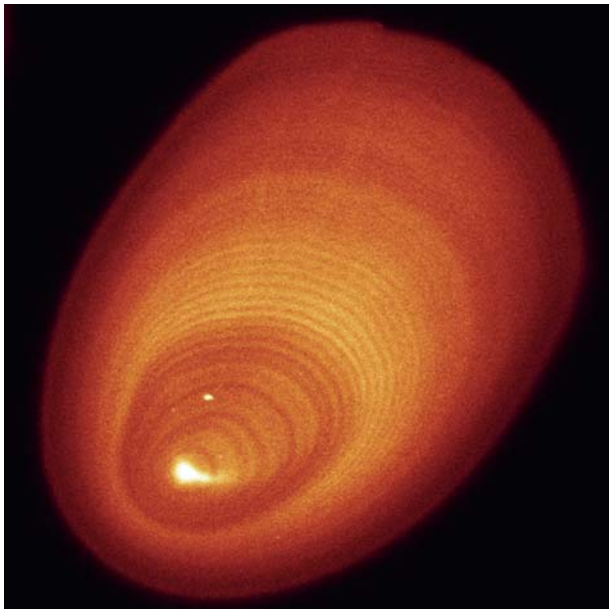

Fig. 4. Higher magnification of an optical CLSM image slice of a normal potato starch granule. Hilum and approx. 1 µm growth ring structures are clearly visible.

polymorph (Imberty et al., 1988a), which is dense, and the B-type polymorph (Imberty, 1988b), which contain water channels. At a yet lower level of organisation, the lamellae may form structures of larger dimensions, which may be related to the growth ring structure of the starch (Gallant et al., 1997; Oostergetel and vanBruggen, 1993).

Genome research programs have now produced a number of plants with specifically altered starch metabolism (Kossman and Lloyd, 2000). These plants offer unique possibilities for detailed investigations of the effects of single genes on the metabolism and deposition of macromolecular structures in the cell. Perturbation of the expression of single genes that are directly involved in starch biosynthesis must inevitably affects the deposition of starch molecules so that normal starch granule formation is impaired. Such deficiencies may then have profound effects on the development of the plant by impaired deposition or immobilisation of starch resulting in limited growth and flowering as demonstrated for plants with impaired starch phosphorylation and degradation (Blennow et al., 2002; Zeeman and apRees, 1999; Yu et al., 2001).

Suppression of the granule bound starch synthase (GBSS) results in the formation of starch granules devoid of amylose (Boyer et al., 1976; Flipse et al., 1996; Fulton et al., 2002; Hylton et al., 1996; Visser et al., 1997) but no effects can be detected on starch granule morphology. However, antisense suppression of soluble starch synthases (SSS), may result in severely misshaped starch granules (Craig et al., 1998; Edwards et al., 1999; Lloyd et al., 1999).

The suppression of starch branching enzyme (SBE) in maize (Bhattacharyya et al., 1993; Boyer et al., 1976), pea (Wang et al., 1998), and potato (Jobling et al., 1999; Schwall et al., 2000) has severe effects on the granule morphology resulting in irregular, elongated, multi lobed or fissured shapes. Mutants devoid of starch debranching enzyme deposit very little starch but large amounts of phytoglycogen, a highly branched α-glucan molecule that does not have the capability at all to form semi-crystalline granules (Kubo et al., 1999; Nakamura et al., 1997; Zeeman et al., 1998). These genotypes clearly demonstrate that the chains of the amylopectin molecule must be optimised in order to generate semi-crystalline and ordered starch granules.

Starch phosphorylation occurs along with starch biosynthesis (Nielsen et al., 1994) but the function of starch phosphorylation is not clear (Blennow et al., 2002). Recent data demonstrates the importance of starch phosphorylation for normal starch degradation (Yu et al., 2001). The effects of suppression of the starch phosphorylating enzyme in potato coded by the *GWD* gene in potato (Lorberth et al., 1998; Ritte et al., 2002) or the *SEX1* (starch excess) homologue in *Arabidopsis* (Yu et al., 2001) are complex. In addition to the starch excess phenotype and starch phosphate deficiency observed in plants with suppressed GWD/SEX1 activity, the amylose content is increased and the amylopectin molecular weight is decreased (Viksø-Nielsen et al., 2001).

There is steadily increasing demand for powerful techniques permitting high resolution imaging of native biopolymer structures. Detailed surface structures at down to 1 nm resolution has been visualized using atomic force microscopy (AFM, Baldwin et al., 1998; Krok et al., 2000; Ohtani et al., 2000; Ridout et al., 2002). Scanning electron microscopy (SEM) has permitted detailed morphological characterisation of starch granules (Jane et al., 1994). This technique offers resolution of surface images at the ~10 nm length scale. However, sample preparation, e.g., dehydration for SEM and AFM can be extremely harsh. Low Voltage SEM has been used to generate high quality images of dehydrated starch granular structures (Baldwin et al., 1997). Using environmental SEM (ESEM) (Danilatos, 1988) gaseous water is allowed to surround the sample permitting biological specimens to be imaged without dehydration. Moreover, the sample does not need to be coated with a conducting material.

The determination of the molecular distribution of amylose and amylopectin molecules in the native starch granule concomitant with the analysis of starch granule internal and surface topography is important for our understanding of mechanisms of starch molecular deposition and starch granule biogenesis. The relative molecular positions and interactions of amylose and amylopectin in the starch granule have been estimated using cross-linking reagents and subsequent disruption of the granular structure (Jane et al., 1992; Kasemsuwan, 1994). Low resolution data on granular branch point distribution was obtained using the high specific binding of the α-1,6-glucosidic starch degrading enzyme pullulanase and the α-1,6/α-1,4 glucosidic degrading enzyme glucoamylase, both linked to gold particles, and subsequent detection using immunoelectron microscopy (Atkin et al., 1998). Less specific techniques such as iodine staining and periodic acid/Shiff's reagent (PAS) also permits visualisation of amylose and amylopectin distribution in starch granule at low-resolution (Atkin et al., 1999; Denyer et al., 2001).

Confocal laser scanning microscopy (CLSM) is a powerful imaging technique that has been very useful for structural carbohydrate analysis of e.g., foods (Dürrenberger et al., 2001). For visualisation of starch structures, different fluorophores have been used including acridine orange and congo red (Adler et al., 1994) and Nile Blue A (Baldwin et al., 1994; Lynn and Cochrane, 1997) and merbromin (Huber and BeMiller, 1997). Recently, the use of FITC, rhodamine, and safranin enabled detailed investigations of the growth ring structure of native and gelatinised starch granules (Van de Velde et al., 2002).

The use of 8-amino-1,3,6-pyrenetrisulfonic acid (APTS) or 8-amino-1,3,6-naphthalenetrisulfonic acid (ANTS) has been used successfully for specific labelling of the reducing ends of starch fragments permitting their separation, quantification, molecular analysis, and sensitive detection (O'Shea et al., 1997, 1998). In the present investigation, the starch molecules in transgenic, native and hydrated starch granules were labelled with APTS in situ, enabling imaging of the molar, internal deposition of starch molecules using CLSM. The surface topologies of the starch granules at high resolution were imaged using ESEM. Possible relationships between starch molecular properties and starch granule topography and internal deposition pattern could be formulated by chromatographic analysis of the solubilised and specifically fragmented starch molecules.

2. Materials and methods

2.1. Starch sources and preparation

Potato starch from a line with suppressed levels of the GBSS protein was obtained from Lyckeby Stärkelsen, Sweden). A potato (*Solanum tuberosum*) line (antisense line no 1) derived from c.v. 'Dianella' with suppressed GWD protein was produced as described elsewhere (Viksø-Nielsen et al., 2001). Starch extracted from a potato line (H944-14.5) derived from c.v. 'Dianella' with reduced starch branching enzyme I and II levels was obtained from Danisco Biotechnology, Denmark. *Curcuma zedoaria* plants, normal potato plants, c.v. 'Dianella,' and antisense GWD plants were grown in a greenhouse with supplementing light. Starch was prepared from mature and fresh potato tubers and *Curcuma* rhizomes as described elsewhere (Blennow et al., 1998). The general effects on starch structure for specific antisense suppression of the GBSS, GWD, and SBE enzyme activities are well documented in literature (Flipse et al., 1996; Lorberth et al., 1998; Schwall et al., 2000; Viksø-Nielsen et al., 2001; Visser et al., 1997). In this work, several lines of the antisense GWD and antisense SBE transgenic plants were initially analysed to confirm that the structural alterations were correlated to the degree of enzyme suppression for each construct and subsequently the most suppressed lines were selected for analysis.

2.2. Environmental scanning electron microscopy (ESEM)

The images shown in this paper are of whole starch granules, which have undergone no special sample preparation prior to the ESEM investigation. A small sample of starch granules was placed on a carbon sticker, which was stuck to the sample stage and gently shaken to distribute the starch evenly over the carbon sticker, before it was placed in the sample chamber of the ESEM instrument (XL30 ESEM FEG SEM, FEL Company, Boston) with a beam voltage of 5 keV, working at a gaseous vapour pressure (water vapousr) of 5 Torr.

2.3. Confocal laser scanning microscopy

Starch granules (2 mg) were dispersed in 3 μl of freshly made APTS solution (20 mM 8-amino-1,3, 6-pyrenetrisulfonic acid (APTS, Molecular Probes), dissolved in 15% acetic acid) and 3 μl of 1 M sodium cyanoborohydride was added. The reaction mixture was incubated at 30 °C for 15 h. The granules were washed 5 times with 1 ml of distilled water and finally suspended in 20 μl of 50% glycerol. For microscopy, the starch granules were fixed in an agar-glycerol matrix. A mixture containing 2% agar and 85% glycerol in water was incubated in a boiling water bath for 5 min to melt the agar. After cooling to room temperature 4 μl of this highly viscous solution was added to 1 μl of the starch granule suspension and the sample thoroughly mixed using a plastic pipette tip. The sample was immediately mounted on a glass plate for microscopy.

A confocal laser scanning microscope (TCS SP2, Leica Microsystems, Wetzlar, Germany) was used for the detection of the fluorescence signal from stained starch grains. The instrument was equipped with an argon laser, the following objective: 40× plan apo/ 1.25–0.75 oil CS, and a spectral filtering system allowing free selection of which intervals of wavelengths to be detected. The filter setting was as follows: excitation wavelength: 488 nm, beam splitter: TD 488/543/ 633, light was detected at the interval from 500 to 535 nm.

For each starch grain a stack of horizontal optical sections was obtained. The stack encompassed the whole grain in three dimensions. The format of the stack was the following: Horizontal direction: 30×30 μm, 512×512 pixels; vertical direction: 5 optical sections per μm. During image acquisition each line was scanned 8 times and averaged to reduce noise. Surfaces of the starch grains could be visualised using simulated fluorescence process projections (SFP, Leica TCS SP2 manual). 3D-image analysis was performed with the software of the TCS SP2. Measurements of the fluorescence intensity were made with Image-Pro Plus (version 4.5, Media Cybernetics, Leiden, The Netherlands).

2.4. Light microscopy

Starch grain suspensions in water were stained with I_2KJ solutions and observed with a light microscope (Zeiss, Oberkochen, Photomikroskop II). Unstained suspensions were subject to polarization microscopy (Leitz, SM-Lux-Pol, Leica Microsystems, Wetzlar,

Germany) Polmi. Starch grains are birefringent showing a Maltese cross on a black background when placed between crossed polarizing filters (oriented west–east and north–south, respectively). The λ-retardation plate was placed in northeast–southwest direction generating birefringent structures that are bright blue or yellow on a pink background dependent on their axis, oriented parallel (blue), or perpendicular (yellow) to the λ-plate.

2.5. Starch molecular analyses

Size exclusion chromatography with refractive index detection (SEC/RI) and high performance anion exchange liquid chromatography/pulsed amperometric detection (HPAEC/PAD) (Blennow et al., 1998) was performed as described elsewhere (Blennow et al., 2001). Amylose content was estimated from the SEC elution profiles as described (Blennow et al., 2001). An APTS

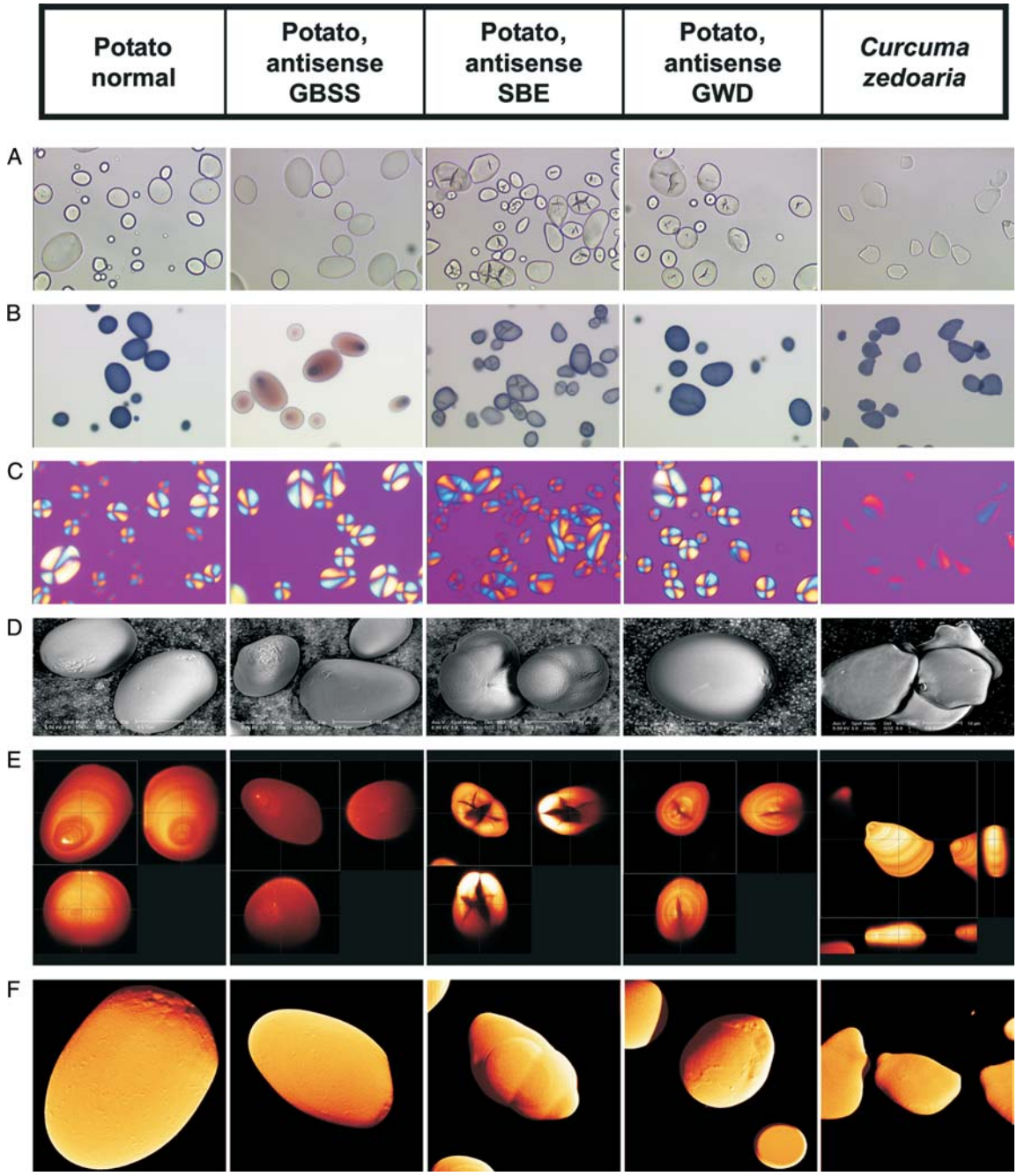

Fig. 2. Images of different normal and transgenically modified starch granules. (A) Brightfield light mictroscopy, (B) Brightfield light mictroscopy iodine staining, (C) Brightfield light mictroscopy polarised light, (D) ESEM, (E) CLSM optical slices, and (F) CLSM surface images. Arrows: CLSM optical slice: amylose rich hilum, CLSM surface image, and ESEM image: "rough areas."

labelled starch sample from the potato control line was subjected to SEC/RI as described above and fractions (2 ml) were collected and the APTS fluorescence analysed using a Perkin–Elmer LS 50B Luminiscence Spectrometer fluorometer (Perkin–Elmer, CT, USA).

3. Results

3.1. Microscopy

Topographical-, internal structural-, and starch molecular distribution analyses of native and transgenically modified storage starch preparations were collected using the combination of three independent and complementary imaging techniques, light microscopy, environmental scanning electron microscopy (ESEM), and confocal laser scanning microscopy, (CLSM, Fig. 2).

3.2. Light microscopy

Light microscopy provides a general characterisation of the granular morphology, starch molecular direction (polarised light) and long-range amylose distribution, and content (iodine staining). Specific differences between the starches could be visualised using light microscopy (Figs. 2A and B). Using brightfield microscopy, fissures and cracks were detected in the antisense SBE and the antisense GWD starch granules. Using polarised light for the same slide a birefringence (''Maltese cross'') effect is clearly visualised (Fig. 2C). Being blue in the northeast and southwest sector, and yellow in the northwest and southeast sector, the birefringent structures in the starch grains are positively birefringent, i.e., the structures have a radial orientation. However, the *C. zedoaria* starch molecules are oriented from a point at the edge of the flattened granules rather than from the centre of the granules. The cracks do not result in a dramatic change in form of the birefringence pattern as indicated in the severely fissured antisense SBE granules. Hence, growth of these granules most likely continues at the surface of the granule after cracking. The birefringence of the antisense SBE granules and the *C. zedoaria* granules is considerably weaker as resulting in a lower contrast between birefringence and background compared to the wild type. This effect would likely be a result of the high amylose (low amylopectin) concentrations of these starch granules since amylose molecules are not expected to be specifically uniformly oriented in the granule. The weak birefringence of the *C. zedoaria* granules indicates the presence of variations in the molecular orientation of the molecules in the starch granules that is not necessarily manifested in granule fissuring since these granules do not show cracks. However, not only the amylopectin content but also the degree of amylopectin disorder seems to vary between the different starches. This is demonstrated for the anti GWD granules which have significantly increased amylose content (Table 1) but similar birefringence to the normal potato granules (Fig. 2C). Unlike the amylose-containing granules, the antisense GBSS granules stain pale purple with iodine revealing their low amylose content. However, at the hilum core, high local concentrations of amylose were detected. Low amylose content did not affect starch granule morphology. The extent of deposition of amylose in the granule core during granule development has been characterised more extensively elsewhere (Tatge et al., 1999).

3.3. ESEM

ESEM provides detailed high-resolution images of starch granular topography in its hydrated state. Most of the starch granules displayed a very smooth surface. The only exception was the antisense SBE granules, which had rough surface properties. These granules also show multilobed granules and the apparent internal fissures observed in light microscopy, were in the ESEM images often shown to be exposed at the surface. The results indicate that the molecular deposition of the starch molecules varies over different regions of the granule. This technique also provides clear images of the ''rough'' and ''smooth'' areas at the surface as described (Baldwin et al., 1998) using atomic force microscopy (AFM). The rough areas or areas with extending lobes are here clearly visible at the end of starch potato starch granules (Fig. 2D). However, it is not clear from these images how the topographic features relate to the inner structures of the starch granule e.g., the position of the hilum.

3.4. CLSM of APTS-labelled starch granules

While ESEM is superior at providing topographical data of the exposed surfaces of the starch granules, CLSM gives a much more comprehensive view of the internal granular structures. Hence, these imaging technologies are highly complementary. A new method was developed where each starch molecule was labelled with the fluorophore APTS in a nearly 1:1 stoichoimetry. Hence, the molecular distribution of the starch molecules is simultaneously indicated.

The same starch samples as subjected to light microscopy and ESEM were investigated with CLSM (Fig. 2). Labelling with APTS is an inherently very efficient reaction (an average of 80% molar labelling efficiency for long α-glucan chains, and close to 100% efficiency for short chains, (O'Shea et al., 1998). Hence, since the fluorophore specifically and with high efficiency reacts with the anomeric carbon at each starch molecule the molar distribution of starch molecules packed in the starch granule is indicated in the CLSM images.

Table 1
Amylose content of the starches as determined size exclusion chromatography, content of mono esterified phosphate and the intensity of fluorescence in cross-sections of CLSM images of starch granules (mean of five determinations)

Sample	Amylose content*(%)	Phosphate content (nmol G6P/mg starch)	Fluorescence intensity** (arbitrary units)
Normal potato	22.2	13.7	27 (4)
High amylopectin potato	2.1	18.1	19 (4)
High amylose potato	40.4	63.5	97 (20)
Low phosphate potato	35.4	1.1	54 (13)
Curcuma zedoaria	41.8	58.8	168 (14)

* As determined from the SEC/RI profiles.
** Parenthesis: SE from 5 independent measurements.

Amylose, being a much smaller molecule than amylopectin, contains a much higher molar ratio of reducing ends per anhydrous glucose residue than the amylopectin molecules resulting in a higher by-weight labelling of amylose. Hence, starch extracted from tubers with low amylose contents (i.e., antisense of granule bound starch synthase, GBSS) showed very little APTS fluorescence and starch granules with low molecular weight amylopectin and/or high amylose contents showed high fluorescence (Table 1). Thus, the APTS fluorescence intensity and the apparent molecular weight of the starch molecules as determined by size exclusion chromatography were positively correlated (Table 1, Figs. 3A–E). The partitioning of label between amylose and amylopectin was further studied by solubilisation of the labelled starch granules and separation of the starch molecules by size exclusion chromatography (Blennow et al., 2001). Subsequent analysis of eluted labelled carbohydrate demonstrates that amylose preferably is labelled (Fig. 3F). This is in agreement with the the above argument that the label is close to equimolar. Hence, using this technology the molar distribution of amylose is efficiently visualised in the in the granules as a result of its much lower molecular mass. Moreover, the growth ring structures were sharper in granules with normal or high amylose contents. This is in agreement with the supposed predominant deposition of amylose in the amorphous growth rings and to a lesser extent in the crystalline growth rings (Montgomery and Senti, 1958). Amylose was also most often detected in a specific layer between the hilum and the surface which is in agreement with findings in maize and potato granules investigated with enzyme gold labelling (Atkin et al., 1999). However, normal and low amylose granules showed an intense approx. 1 μm large fluorescence dot in the hilum indicating a high concentration of amylose in the centre of the granule in agreement with the iodine stained anti GBSS granules. The growth ring structure, deposition pattern of amylose and hilum is clearly visualised in Fig. 4.

By the combination of CLSM and ESEM, the position of the ''rough areas'' visualised by ESEM could be localised at the opposite end as the hilum (Figs. 2D–F). The protrusions at the surface may indicate irregular packing of the starch molecules in these regions.

However, it was not possible to indicate any changes in fluorescence or birefringence specific for the rough regions. The region of the starch granule between hilum and the surface has in this case very thin or invisible (unresolved) ring structures.

Starch granules with suppressed starch branching enzyme (SBE) had severe internal cracks and rough surfaces (Fig. 2D). This starch has high phosphate and amylose content (Fig. 3C, Table 1) and long amylopectin side chains (Fig. 5C). The starch prepared from *C. zedoaria* has naturally high starch phosphate content and high amylose content (Table 1) but the starch granules show no fissures and they have a smooth surface (Fig. 2). Hence, from these data no clear conclusions of the exclusive impact of phosphate, amylose or long amylopectin side chains on granule morphology and topography can be made.

Antisense of the GWD enzyme resulted in severely reduced starch phosphate concentration in the starch (Table 1), a high proportion of low molecular weight amylopectin (Fig. 3D) and fissures in the granules (Fig. 2). These fissures were not as severe as those found in the antisense SBE starch granules. However, occasionally the fissures protrude at the surface of the starch granule (Fig. 2E). No extremely long amylopectin chains were found in this type of starch. The observed fractures may be effects of long-range destabilisation due to the severely reduced phosphate content, its high amylose content, the low molecular weight amylopectin or combinations of these structural parameters.

The possible contribution of structural parameters for starch granule integrity is discussed in more detail below.

4. Discussion

The possible effects of amylose and amylopectin concentrations and structure and esterified phosphate content on starch granule morphology, topography, and starch molecular deposition was investigated using a

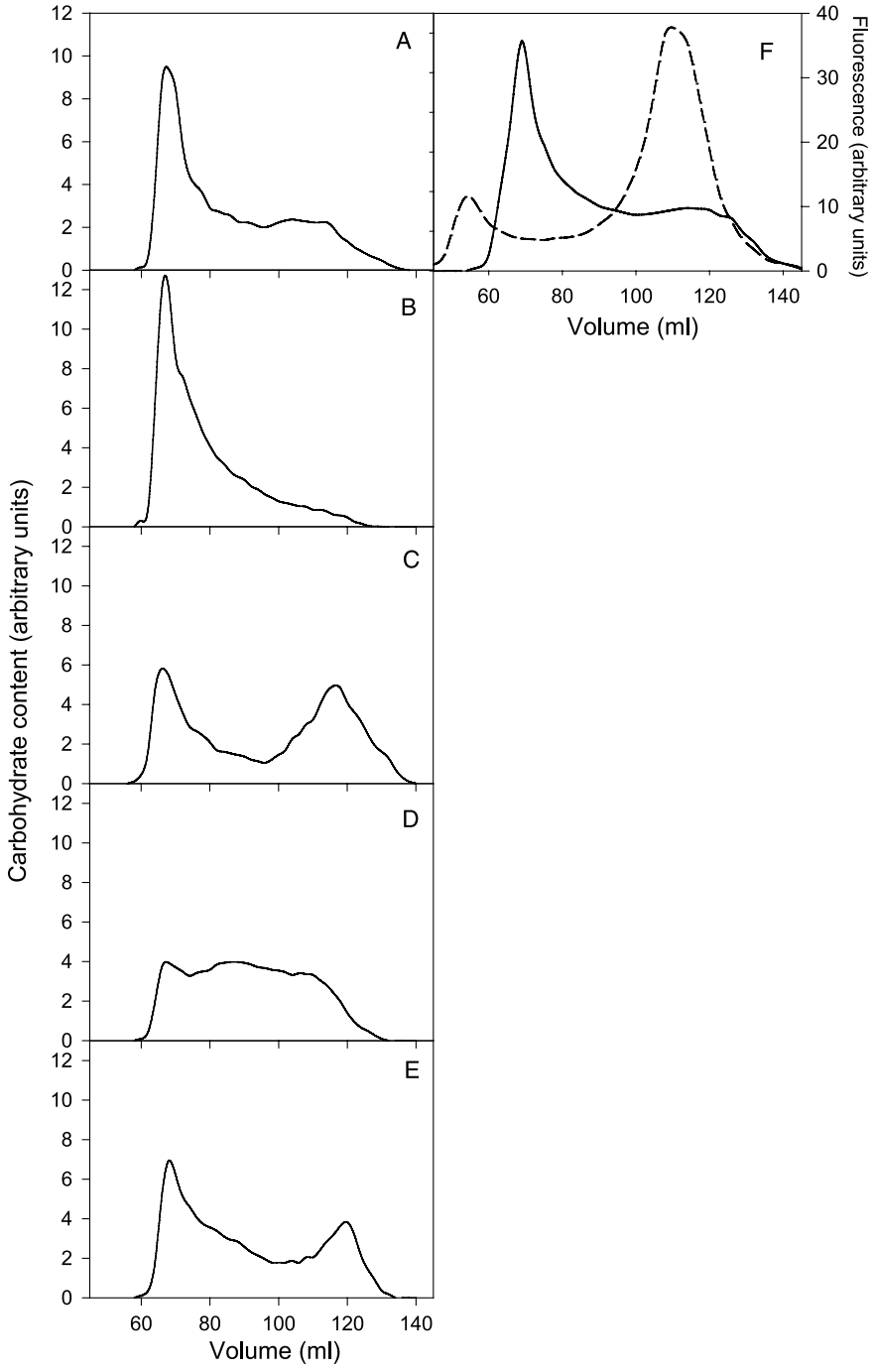

Fig. 3. SEC-RI analysis of starch extracted from (A) normal potato (B) potato antisense GBSS, (C) potato antisense SBE, (D) potato antisense GWD, (E) *C. zedoaria*, and (F) size exclusion chromatographic (SEC) analysis of starch extracted from normal potato starch labelled with APTS. (line: carbohydrate content, dotted line: APTS fluorescence intensity, arbitrary units).

bioimaging approach. Bioimaging offers the possibility to obtain data for single granules and in the case of the novel CLSM technique, relative values of the deposition of amylose and/or low Mw amylopectin starch molecules are estimated. Hence, the variation within a granular population can be assessed. Moreover, preliminary experiments indicate that APTS quite specifically labels starch granules and to a lesser extent cell walls in tissue that has been extracted with ethanol. Hence, using CLSM in combination with APTS labelling, the molecular mechanisms of starch deposition and remobilisation can in principle be monitored in situ. Changed flow of carbon through the different starch biosynthetic enzyme pathways will alter structural motifs of the starch. Hence, by studying transgenic starch granule preparations, the imaging data can be correlated

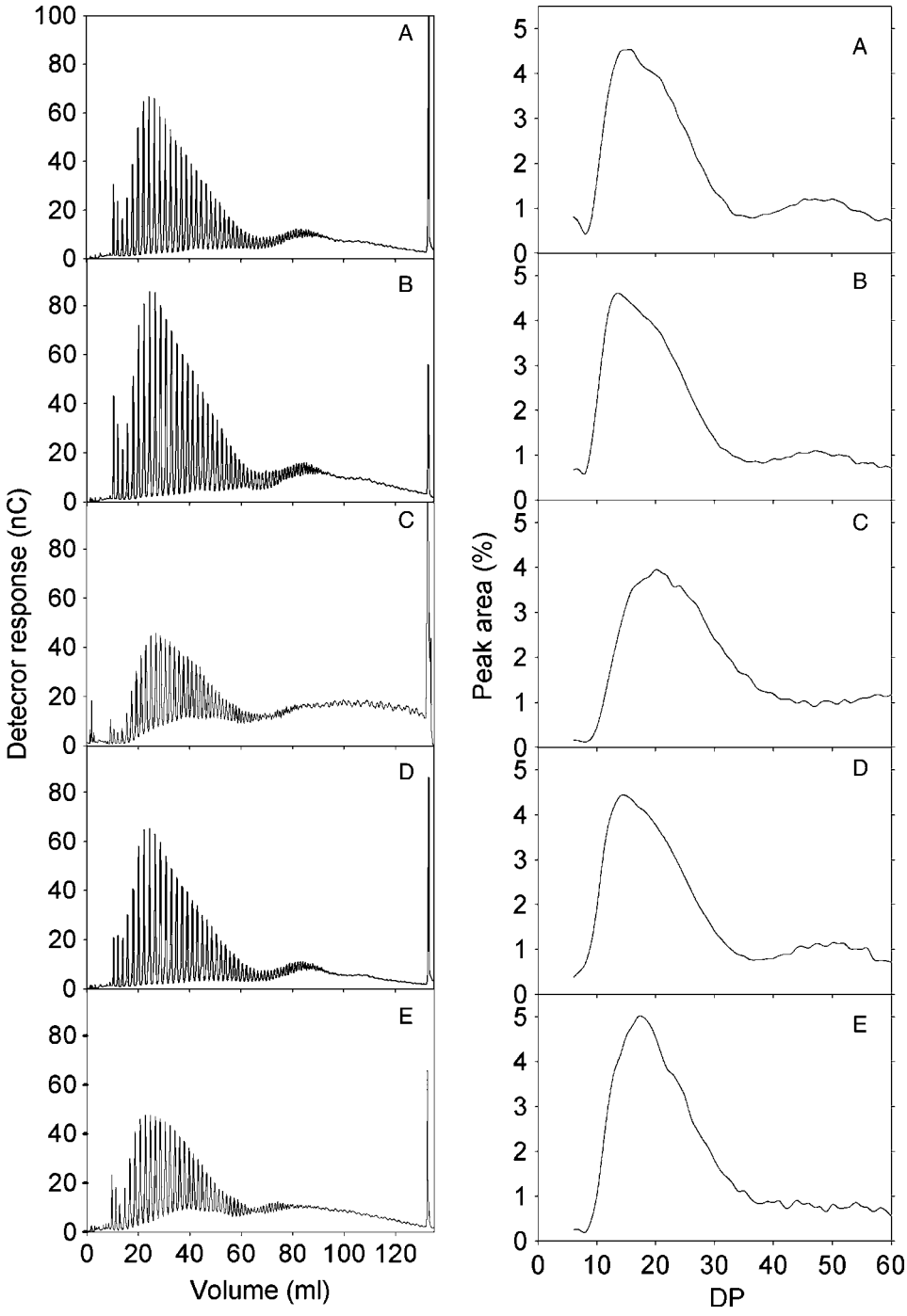

Fig. 5. HPAEC/PAD chromatography of amylopectin unit chains: (A) Normal potato, (B) potato antisense GBSS, (C) potato antisense SBE, (D) potato antisense GWD, and (E) *C. zedoaria*. (Left) Raw chromatograms. (Right) Integrated single peaks of chains between DP 6 and DP 60. The areas of the peaks were corrected for variations in detector response (Blennow et al., 1998) and the relative concentration for each peak plotted (total corrected peak area = 100%).

to single starch metabolic reactions. However, since the effects of suppression of a single enzyme activity often have multiple (pleiotropic) effects on starch metabolism as exemplified in this work, even though these effects seem to be less significant for alterations of starch metabolism in the potato tuber compared to e.g., endosperm, unequivocal links between starch structure and morphology are hard to estimate. However, important data can be collected and evaluated indicating the effects of possible structural motifs.

The most likely source of alterations on the starch granule morphology is the effects of "non-structurable"

amylopectin chains generating erroneous chain packing in the granule irrespective of the presence of amylose. However, direct amylopectin–amylose interactions can be detrimental for normal starch granule formation. At low and normal concentrations, amylopectin structure is not significantly altered by the presence of amylose based on that the amylose molecules are possibly synthesised and deposited in existent small cavities in the starch granules (Denyer et al., 2001; Tatge et al., 1999). However, amylose has been suggested to disrupt structural order to some degree within the crystalline amylopectin molecular arrays either by direct intermolecular double helical formation within the amylopectin crystalline lamellae or by reinforcing the amorphous amylopectin lamella (Jenkins and Donald, 1995) which may in extreme cases result in granule disruption. Amylose–amylopectin double helical interactions would be favoured where amylopectin with long chains and/or amylose with many branch points are simultaneously synthesised in close proximity to each other. Hence, in order to avoid cracking, amylose and amylopectin have to be significantly different in structure. ''Amylopectin-like amylose'' or ''amylose-like amylopectin'' would distort starch granule integrity. The fact that starch granules that are composed of pure amylopectin do not readily crack points at a significant disturbing effect of amylose. It is feasible to consider that amylose and amylopectin are efficiently phase separated during biosynthesis of the granule. Such separation can be demonstrated in vitro for amylose–amylopectin mixtures (Kalichevski and Ring, 1987; Rindlav-Westling et al., 2002). Phosphate esterified to the amylopectin chains most possibly affects interactions involved in this phase partitioning.

The effects on starch granule morphology of amylose–amylopectin interactions have been indicated by the severely misshaped starch granules starch granules synthesised in potato tubers with antisense suppressed soluble starch synthase (SSS) activity (Craig et al., 1998; Edwards et al., 1999; Lloyd et al., 1999). Very long side chains in the amylopectin was observed in this line. The simultaneous suppression of SSS and GBSS caused a reversion to the original morphology of the starch granules indicating that the presence of amylose can have detrimental effects in granules with erroneous amylopectin structure (Fulton et al., 2002). Since no very long amylopectin chains were detected in the double mutant, it was proposed that these chains might be responsible for the observed cracking in the antisense SSS line, possibly by interaction with non-structured amylose.

The effect of phosphate is less clear. Hypothetically, the presence of phosphate in amylopectin might serve to partition the non-phosphorylated and unstructured amylose away from the amylopectin crystalline arrays and thus prevent amylose–amylopectin interactions. Such interactions would be favourable in tuberous starches where the amylopectin side chains are relatively long (Blennow et al., 2000a). In cereal storage starch, amylose is supposedly complexed with phospholipids by inclusion in single helices (Lim et al., 1994). This complexation would help to partition the amylose away from the non-phosphorylated amylopectin in the cereal starch system. For potato and wheat starch a significant difference has been found with respect to the compatibility between their amylose and amylopectin fractions, respectively, (Svegmark and Hermansson, 1991). Wheat amylose and amylopectin was shown to be less compatible than potato amylose and amylopectin suggesting that the extent of structural difference between these two macromolecules e.g., phosphate esters or branch lengths can significantly affect amylose–amylopectin interactions.

Although as indicated by preliminary molecular models of phosphorylated starch (Blennow et al., 2002) there is no exclusive evidence for a significant destabilising effect of a high phosphate content on molecular packing of the amylopectin chains. Phosphate may alternatively serve as a plastiziser, ''stabiliser'' or ''filler'' between double helical mesogens providing attractive forces in the granule lamellar organisation where local irregularities are present. This situation can arise when the helix mesogens cannot align perfectly parallell.

Starches extracted from two of the genotypes in this investigation, the antisense SBE and the antisense GWD potato lines, showed fissures or cracks indicating sub-optimal packing of the starch molecules in the starch granules. The reason for this is not obvious but can be addressed by comparison of the different starch granule types investigated in this and other studies. In analogy with the long amylopectin chains found in the fissured antisense SSS starch granules, it can be argued that the long unit chains of amylopectin (>DP 100) detected by HPAEC in the amylopectin molecules of the SBE antisense line in the present investigation would favour amylopectin–amylose double helical interactions provided that a large proportion of these chains are outer chains. This could result in incorrect crystallisation of the amylopectin double helices and subsequent cracking. However, for this starch the amylopectin chain structure could, independently of the presence of amylose, result in sub optimal chain packing. The recent model of the starch granule at the nanoscale requires the amylopectin mesogens to be optimally registered and to have reasonably constant length scales. Large deviations are not permitted. Since a crystalline lamella being 5–7 nm in length would be built from chain pools of approx. DP 14–20, significant amounts of chains longer than approx. DP20 will exceed the proposed crystalline double helical lamellar dimension and hence destroy the optimal packing of double helical segments.

Similar fissures were found in the granules synthesised by the GWD antisense genotype. However, no increased amounts of long amylopectin side chains were found in these starch samples (Fig. 5D). In contrast to the other starches, the amylose and amylopectin of this line were not readily separated by SEC indicating that this starch has a very low molecular weight amylopectin and a rather high molecular weight amylose. The reason for fissuring may thus be similar to the case for the anti SBE starch granules since high molecular weight amylose has been shown to contain more branch points than low molecular weight amylose (Cheetham and Tao, 1997; Mua and Jackson, 1997), This type of amylose would favour amylose–amylopectin interaction by providing amylopectin-like flexible short chain segments in the amylose molecules. It may also be argued that amylopectin with low molecular weight would not be capable of keeping the granule intact, especially in cases where minor stress is built in during biosynthesis of the granule as indicated by the appearance of concave surfaces obtained after mechanical sectioning (Ridout et al., 2002; Whitworth et al., 1998). Since the amylopectin of this starch contains very little covalently linked phosphate, the amylose and amylopectin fractions in these starch granules are similar which may in principle favour intermolecular amylose–amylopectin interactions.

Finally, the *C. zedoaria* starch granules have no cracks despite the presence of high amylose concentration in these granules. However, these granules are composed of low molecular weight amylose and highly phosphorylated amylopectin that may not allow extensive amylose–amylopectin interactions as discussed above. Again, this indicates that phosphorylation of long AP chains can be a mechanism for the plant to prevent such interactions. The flat, quasi 2D shape of these granules may reduce strain normally developed during starch granule growth and hence prevent cracking.

5. Conclusions

The combined molecular structural and bioimaging analysis of transgenic starches has allowed several coordinated mechanisms behind starch granule morphogenesis to be envisioned. It can be hypothesised that the branch length, molecular weight, and phosphate substitution of the starch molecules would play significant roles for correct amylopectin double helix formation and crystallisation during granule morphogenesis.

Acknowledgments

This research was supported by The Danish National Research Foundation, The Danish Biotechnology Programme and the Danish Directorate for Development (non-food and Centre for Development of Improved Food Starches), The Commitee for Research and Development of the Öresund Region (Öforsk) and an EU Marie Curie PhD stipend. We thank Lis B. Møller and Helle K. Mogensen for technical assistance. Lyckeby Stärkelsen, Sweden is thanked for the potato high amylopectin potato starch and KMC a.m.b.a., Denmark for providing the normal potato starch.

References

Adler, J., Baldwin, P.M., Melia, C.D., 1994. Starch damage part 2: Types of damage in ball-milled potato starch, upon hydration observed by confocal microscopy. Starch Staerke 46, 252–256.

Atkin, N.J., Cheng, S.L., Abeysekera, R.M., Robards, A.W., 1999. Localisation of amylose and amylopectin in starch granules using enzyme-gold labelling. Starch Staerke 51, 163–172.

Atkin, N.J., Cheng, S.L., Abeysekera, R.M., Robards, A.W., 1998. The events leading to the formation of ghost remnants from the starch granule surface and the contribution of the granule surface to the gelatinization endotherm. Carbohydr. Polym. 36, 193–204.

Baldwin, P.M., Adler, J., Davies, M.C., Melia, C.D., 1994. Holes in starch granules: Confocal, SEM and light microscopy studies of starch granule structure. Starch Staerke 46, 341–346.

Baldwin, P.M., Adler, J., Davies, M.C., Melia, C.D., 1998. High resolution imaging of starch granule surfaces by atomic force microscopy. J. Cereal Sci. 27, 255–265.

Baldwin, P.M., Davies, M.C., Melia, C.D., 1997. Starch granule surface imaging using low-voltage scanning electron microscopy and atomic force microscopy. Int. J. Biol. Macromol. 21, 103–107.

Bhattacharyya, M., Martin, C., Smith, A., 1993. The importance of starch biosynthesis in the wrinkled weed shape character. Plant Mol. Biol. 22, 525–531.

Blennow, A., Engelsen, S.B., Nielsen, T.H., Baunsgaard, L., Mikkelsen, R., 2002. Starch phosphorylation—a new front line in starch research. Trends Plant Sci. 7 (9), 445–450.

Blennow, A., Bay-Smidt, A.M., Olsen, C.E., Møller, B.L., 1998. Analysis of starch-bound glucose 3-phosphate and glucose 6-phosphate using controlled acid treatment combined with high-performance anion-exchange chromatography. J. Chromatogr. A 829, 385–391.

Blennow, A., Engelsen, S.B., Munck, L., Møller, B.L., 2000a. Starch molecular structure and phosphorylation investigated by a combined chromatographic and chemometric approach. Carbohydr. Polym. 41, 163–174.

Blennow, A., Bay-Smidt, A.M., Olsen, C.E., Møller, B.L., 2000b. The distribution of covalently bound phosphate in the starch granule in relation to starch crystallinity. Int. J. Biol. Macromol. 27, 211–218.

Blennow, A., Bay-Smidt, A.M., Bauer, R., 2001. Amylopectin aggregation as a function of starch phosphate content studied by size exclusion chromatography and on-line refractive index and light scattering. Int. J. Biol. Macromol. 28, 409–420.

Boyer, C.D., Daniels, R.R., Shannon, J.C., 1976. Abnormal starch granule formation in the Zea mays L. endosperms possessing the amylose-extender mutant. Crop Sci. 16, 298–301.

Buléon, A., Colonna, P., Planchot, V., Ball, S., 1998. Starch granules: structure and biosynthesis. Int. J. Biol. Mol. 23, 85–112.

Cheetham, N.W.H., Tao, L., 1997. The effects of amylose content on the molecular size of amylose, and on the distribution of amylopectin chain length in maize starches. Carbohydr. Polym. 33, 251–261.

Craig, J., Lloyd, J.R., Tomlinson, K., Barber, L., Edwards, A., Wang, T.L., Martin, C., Hedley, C.L., Smith, A.M., 1998. Mutations in the gene encoding starch synthase II profoundly alter amylopectin structure in pea embryos. Plant Cell 10, 413–426.

Danilatos, G.D., 1988. Foundations of environmental scanning electron-microscopy. Adv. Electron. Electron Phys. 71, 109–250.

Denyer, K., Johnson, P., Zeeman, S., Smith, A.M., 2001. The control of amylose synthesis. J. Plant Physiol. 158, 479–487.

Dürrenberger, M.B., Handschin, S., Conde-Petit, B., Escher, F., 2001. Visualization of food structure by confocal laser light scanning microscopy (CLSM). Lebensm. Wiss. Technol. 34, 11–17.

Edwards, A., Fulton, D.C., Hylton, C.M., Jobling, S.A., Gidley, M.J., Rössner, U., Martin, C., Smith, A.M., 1999. A combined reduction in activity of starch synthases II and III of potato has novel effects on the starch of tubers. Plant J. 17, 251–261.

Flipse, E., Keetels, C., Jacobsen, E., Visser, R.G., 1996. The dosage effect of the wildtype GBSS allele is linear for GBSS activity. Theor. Appl. Genet. 92, 121–127.

Fulton, D.C., Edwards, A., Pilling, E., Robinson, H.L., Fahy, B., Seale, R., Donald, A.M., Geigenberger, P., Martin, C., Smith, A.M., 2002. Role of granule bound starch synthase in determination of amylopectin structure and starch granule morphology in potato. J. Mol. Biol. 277, 10834–10841.

Gallant, D.J., Bouchet, B., Baldwin, P.M., 1997. Microscopy of starch: evidence of a new level of granule organization. Carbohydr. Polym. 32, 177–191.

Huber, K.C., BeMiller, J.N., 1997. Visualization of channels and cavities of corn and sorghum starch granules. Cereal Chem. 74, 537–541.

Hylton, C.M., Denyer, K., Keeling, P.L., Chang, M.T., Smith, A.M., 1996. The effect of waxy mutations on the granule-bound starch synthases of barley and maize endosperms. Planta 198, 230–237.

Imberty, A., Chanzy, H., Pérez, S., Buléon, A., Tran, V., 1988a. The double-helical nature of the crystalline part of A-starch. J. Mol. Biol. 201, 365–378.

Imberty, A., Pérez, S., 1988b. A revisit to the three-dimensional structure of B-type starch. Biopolymers 27, 1205–1221.

Jane, J.L., Kasemsuwan, T., Leas, S., Zobel, H., Robyt, J., 1994. Anthology of starch granule morphology by scanning electron microscopy. Starch Staerke 46, 121–129.

Jane, J., Xu, A., Radosavljevic, M., Seib, P.A., 1992. Location of amylose in normal starch granules. 1. Susceptibility of amylose and amylopectin to cross-linking reagents. Cereal Chem. 69, 405–409.

Jenkins, P.J., Cameron, R.E., Donald, A.M., 1993. A universal feature in the structure of starch granules from different botanical sources. Starch Staerke 45, 417–420.

Jenkins, P.J., Donald, A.M., 1995. The influence of amylose on starch granule structure. Int. J. Biol. Macromol. 17, 315–321.

Jobling, S.A., Schwall, G.P., Westcott, R.J., Sidebottom, C., Debet, M., Gidley, M.J., Jeffcoat, B., Safford, R., 1999. A minor form of starch branching enzyme in potato (*Solanum tuberosum* L.) tubers has a major effect on starch structure: cloning and characterisation of multiple forms of SBE A. Plant J. 18, 163–171.

Kalichevski, M.T., Ring, S.G., 1987. Incompatibility of amylose and amylopectin in aqueous solution. Carbohydr. Res. 162, 323–328.

Kasemsuwan, T., 1994. Location of amylose in normal starch granules. 2. Locations of phosphodiester cross-linking revealed by phosphorus-31 nuclear magnetic resonance. Cereal Chem. 71, 282–287.

Kossman, J., Lloyd, J., 2000. Understanding and influencing starch biochemistry. Crit. Rev. Plant Sci. 19, 171–226.

Krok, F., Szymo'nska, J., Tomasik, P., Szymo'nski, M., 2000. Non-contact AFM investigation of influence of freezing process on the surface structure of potato starch granule. Appl. Surface Sci. 157, 382–386.

Kubo, A., Fujita, N., Harada, K., Matsuda, T., Satoh, H., Nakamura, Y., 1999. The starch-debranching enzymes isoamylase and pullulanase are both involved in amylopectin biosynthesis in rice endosperms. Plant Physiol. 121, 399–409.

Lim, S.T., Kasemsuwan, T., Jane, J.L., 1994. Characterization of phosphorous in starch by 32P-nuclear magnetic resonance spectroscopy. Cereal Chem. 71, 488–493.

Lloyd, J.R., Landschütze, V., Kossmann, J., 1999. Simulaneous antisense inhibition of two starch-synthase isoforms in potato tubers leads to accumulation of grossly modified amylopectin. Biochem. J. 338, 515–521.

Lorberth, R., Ritte, G., Willmitzer, L., Kossmann, J., 1998. Inhibition of a starch-granule-bound protein leads to modified starch and repression of cold sweetening. Nat. Biotech. 16, 473–477.

Lynn, A., Cochrane, M.P., 1997. An evaluation of confocal microscopy for the study of starch granule enzymic digestion. Starch Staerke 49, 106–111.

Manners, D.J., 1989. Recent developments in our understanding of amylopectin structure. Carbohydr. Polym. 11, 87–112.

Montgomery, E.M., Senti, F.R., 1958. Separation of amylose from amylopectin of starch by an Extraction-sedimentation procedure. J. Polym. Sci. 28, 1–9.

Mua, J.P., Jackson, D.S., 1997. Fine structure of corn amylose and amylopectin fractions with various molecular weights. J. Agric. Food Chem. 45, 3840–3847.

Muhrbeck, P., Svensson, E., Eliasson, A-.C., 1991. Effect of the degree of phosphorylation on the crystallinity of native potato starch. Starch Staerke 43, 466–468.

Nakamura, Y., Kubo, A., Shimamune, T., Matsuda, T., Harada, K., Satoh, H., 1997. Correlation between activities of starch debranching enzyme and α-polyglucan structure in endosperms of sugary-1 mutants of rice. Plant J. 12, 143–153.

Nielsen, T.H., Wischmann, B., Enevoldsen, K., Møller, B.L., 1994. Starch phosphorylation in potato tubers proceeds concurrently with de novo biosynthesis of starch. Plant Physiol. 105, 111–117.

Obanni, M., BeMiller, J.N., 1997. Properties of some starch blends. Cereal Chem. 74, 431–436.

Ohtani, T., Yoshino, T., Hagiwara, T., Maekawa, T., 2000. High-resolution imaging of starch granule structure using atomic force microscopy. Starch Staerke 52, 150–153.

Oostergetel, G.T., vanBruggen, E.F.J., 1993. The crystalline domains in potato starch granules are arranged in a helical fashion. Carbohydr. Polym. 21, 7–12.

O'Shea, M.G., Morell, M.K., 1997. High resolution slab gel electrophoresis of 8-amino-1,3,6-pyrenetrisulfonic acid (APTS) tagged oligosaccharides using a DNA sequencer. Electrophoresis 17, 681–688.

O'Shea, M.G., Samuel, M.S., Konik, C.M., Morell, M.K., 1998. Flourophore-assisted carbohydrate electrophoresis (FACE) of oligosaccharides:efficiency of labelling and high-resolution separation. Carbohydr. Res. 307, 1–12.

Ridout, M.J., Gunning, A.P., Parker, M.L., Wilson, R.H., Morris, V.J., 2002. Using AFM ti image the internal structure of starch granules. Carbohydr. Polym. 50, 123–132.

Rindlav-Westling, Å., Stading, M., Gatenholm, P., 2002. Crystallinity and morphology in films of starch, amylose and amylopectin blends. Biomacromolecules 3, 84–91.

Ritte, G., Lloyd, J.R., Eckermann, N., Rottmann, A., Kossmann, J., Steup, M., 2002. The starch-related R1 protein in an α-glucan, water dikinase. PNAS 99, 7166–7171.

Schwall, G.P., Safford, R., Westcott, R.J., Jeffcoat, B., Tayal, A., Shi, Y.-C., Gidley, M.J., Jobling, S.A., 2000. Production of very-high-amylose potato starch by inhibition of SBE A and B. Nat. Biotechnol. 18, 551–554.

Smith, A.M., 2001. The Biosynthesis of starch granules. Biomacromolecules 2, 335–341.

Svegmark, K., Hermansson, A.-M., 1991. Distribution of amylose and amylopectin in potato starch pastes: effects of heating and shearing. Food Struct. 10, 117–129.

Tatge, H., Marchall, J., Martin, C., Edwards, A., Smith, A.M., 1999. Evidence that amylose synthesis occurs within the matrix of the starch granule in potato tubers. Plant Cell Env. 22, 543–550.

Van de Velde, F., van Riel, J., Tromp, R.H., 2002. Visualisation of starch granule morphologies using confocal. J. Sci. Food Agric. 82, 1528–1536.

Viksø-Nielsen, A., Blennow, A., Jørgensen, K., Kristensen, K.H., Jensen, A., Møller, B.L., 2001. Structural, physicochemical, and pasting properties of starches from potato plants with repressed r1-Gene. Biomacromolecules 2, 836–843.

Visser, R.G.F., Suurs, L.C.J.M., Bruinenberg, P.M., Bleeker, I., Jacobsen, E., 1997. Comparison between amylose-free and amylose containing potato starches. Starch Staerke 49, 438–443.

Waigh, T.A., Perry, P., Riekel, C., Gidley, M.J., Donald, A.M., 1998. Chiral side-chain liquid-crystalline polymeric properties of starch. Macromolecules 31, 7980–7984.

Wang, T.L., Bogracheva, T.Y, Hedley, C.L., 1998. Starch: as simple as A, B, C? J. Exp. Bot. 49, 481–502.

Whitworth, M.B., Evers, T.D., Greenwell, P., 1998. Residual stress: a proposed mechanism for starch granule mechanical properties. (Abstract) ''Production and uses of starch'', Edinburgh, 6–8 April 1998.

Zeeman, S.C., apRees, T., 1999. Changes in carbohydrate metabolism and assimilate export in starch-excess mutants of Arabidopsis. Plant Cell Env. 22, 1445–1453.

Zeeman, S.C., Umemoto, T., Lue, W.L., Au-Yeung, P., Martin, C., Smith, A.M., Chen, J., 1998. A mutant of *Arabidopsis* lacking a chloroplastic isoamylase accumulates both starch and phytoglycogen. Plant Cell 10, 1699–1711.

Yu, T.-S., Kofler, H., Häusler, R.E., Hille, D., Flügge, H.-I., Zeeman, S.C., Smith, A.M., Kossmann, J., Lloyd, J., Ritte, G., Steup, M., Lue, W., Chen, J., Weber, A., 2001. The Arabidopsis sex1 mutant is defective in the R1 protein, a general regulator of starch degradation in plants, and not in the chloroplast hexose transporter. Plant Cell 13, 1907–1918.